PRECISE AIRBORNE LIDAR SURVEYING FOR COASTAL RESEARCH AND GEOHAZARDS APPLICATIONS

Roberto Gutierrez, James C. Gibeaut, Rebecca C. Smyth, Tiffany L. Hepner, John R. Andrews
Bureau of Economic Geology, The University of Texas at Austin, Austin, Texas, USA
oskar@mail.utexas.edu
Christopher Weed
Center for Space Research, The University of Texas at Austin, Austin, Texas, USA
William Gutelius
Optech, Inc., Toronto, Canada
Mark Mastin
U.S. Geological Survey, Tacoma, Washington, USA

KEYWORDS: LIDAR, laser, ALSM, calibration, natural hazards, shoreline mapping

ABSTRACT

The monitoring and analysis of many natural hazards requires repeated measurements of a topographic surface whose change reflects some geologic or hydrologic process. The development of airborne laser surface mapping (ALSM) allows the study of natural hazards over areas tens to hundreds of kilometers in extent with a horizontal resolution of 1 meter or less and a vertical accuracy of 0.10-to-0.15m. Change detection requires that repeated ALSM surveys be precise and accurate. Repeatability is a function of the stability and calibration of the instrument, the accuracy of GPS aircraft trajectories, the density and completeness of ALSM data coverage, the availability of "ground truth" information, and the accuracy and flexibility of ALSM data classification. Since 1997 The University of Texas at Austin (UT) has mapped various portions of the Texas Gulf coast using several small-footprint, scanning ALSM systems developed by Optech, Inc. During summer 2000, UT comprehensively mapped the Texas coast from Sabine Pass on the Texas-Louisiana border to the mouth of the Rio Grande River. These data provide a series of Gulf shorelines for estimating beach erosion rates and computing volumetric sand loss. The high-resolution beach and dune topography derived from ALSM will help characterize the susceptibility of the coast to hurricane overwash and storm-related flooding. In another project UT collaborated with Optech and the U.S. Geological Survey in March 2000 to survey fifteen municipalities in Honduras with ALSM as part of the USAID Hurricane Mitch Recovery program. Digital elevation models produced from these data are being used for flood and landslide hazard analysis. During these and other projects, UT began implementing procedures for instrument calibration, data classification, and ground GPS surveying that enhance the repeatability of our ALSM surveys.

1 INTRODUCTION

The Bureau of Economic Geology (BEG), a geologic and environmental research group within the University of Texas at Austin (UT), is the state agency responsible for providing shoreline information to the Texas legislature and state regulatory agencies. Because of the requirement for accurate shoreline data, the BEG began a program in airborne laser surface mapping (ALSM) in collaboration with the UT Center for Space Research, and Optech, Inc. This program began with a shoreline survey in December 1997 using an ALSM system provided by Optech (Gutierrez et al, 1998). In July 2000, UT acquired an Optech ALTM 1225 instrument, a 25kHz scanning laser mapping system. In this paper we describe our current ALSM program and how we are implementing geodetic techniques into our operations. We also discuss some results from our Texas shoreline mapping and a flood-hazard mapping project in Honduras, C.A.

2 METHODS

NASA began developing ALSM technology in the 1980's and several instruments (RASCAL, SLICER, AOL, LVIS, ATM) were developed for terrain, vegetation, and ice sheet mapping (Rabine et al, 1996; Harding et al, 2000; Krabill et al, 1995; Blair et al, 1999, Krabill et al, 2000). Commercial ALSM systems became available as the technology matured. Optech developed the ALTM 1020, a compact scanning ALSM system with a 5kHz laser repetition pulse rate, in 1995. Increases in laser power, laser pulse rate, and overall system performance were incorporated by Optech in subsequent models with the ALTM 1225 system appearing in 1999. The ALTM 1225 has the following specifications:

- Operating altitude 410-2,000 m AGL
- Laser pulse rate 25 kHz
- Laser scan angle variable from 0 to ± 20° from nadir
- Scanning frequency variable, 28 Hz at the 20° scan angle.
- Beam divergence 0.2 milliradian (half angle, 1/e)

The ALTM 1225 does not digitize and record the waveform of the laser reflection, but records the range and backscatter intensity of the first and last laser reflection using a constant-fraction discriminator and two Timing Interval Meters (TIM).

ALSM elevation points are computed using three sets of data: laser ranges and their associated scan angles, platform position and orientation information, and calibration data and mounting parameters (Wehr and Lohr, 1999). Global Positioning System (GPS) receivers in the aircraft and on the ground provide platform positioning. The GPS receivers record pseudo-range and phase information for post-processing. Platform orientation information comes from an Inertial Measurement Unit (IMU) containing three orthogonal accelerometers and gyroscopes. An aided-Inertial Navigation System (INS) solution for the aircraft's attitude is estimated from the IMU output and the GPS information.

2.1 Calibration

There are no standard instrument calibration procedures, each equipment manufacturer and ALSM group have developed its own techniques (Wehr and Lohr, 1999). The instrument calibration for our Optech ALTM 1225 includes the estimation of the scanner roll and pitch bias corrections, a scanner scale correction, and a timing correction for each TIM. These corrections were initially measured in the manufacturer's laboratory facility and refined by flight testing. In the laboratory, range corrections were also tabulated for varying intensities of laser backscatter. We re-estimate the instrument calibration by flight-testing before and after an ALSM survey. Estimating GPS datum or ranging errors requires flying the instrument against "ground truth" - an area (e.g. road or airport runway) surveyed by ground GPS or conventional means. However, the scanner roll, pitch and scale biases can be accurately estimated through the careful comparison of overlapping flightlines (Burman, 2000).

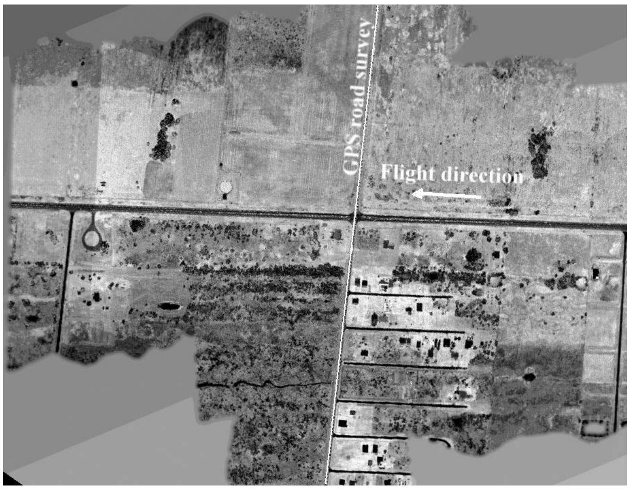

Figure 1. Laser backscatter intensity image of calibration area.

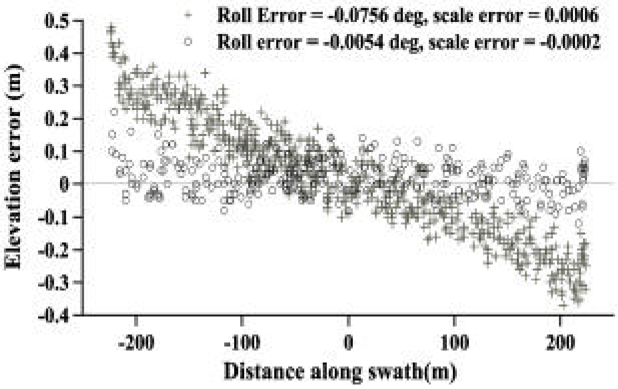

Figure 2. Roll and scale errors before and after adjustment.

Figure 1 is a laser backscatter intensity image constructed from several flightlines on the Texas coast. Indicated on the image is a kinematic GPS ground survey on a paved road oriented normal to the direction of four crossing flightlines. Figure 2 shows the elevation differences (+) between the ground GPS and one of these crossing ALSM flightlines processed using nominal calibration settings. We estimated calibration corrections from four flights spaced over two weeks (July 12 through July 27, 2001) of surveying. Plotted for comparison are the elevation differences (**O**) between the ground GPS and the same flightline after calibration adjustment. The consistency of the four calibration flights indicates that the ALSM system's pointing accuracy has a RMS of ≤0.01° and a scanner scale RMS of ≤0.0006.

2.2 GPS

The absolute positioning of the ALSM platform comes from GPS. Therefore planning the GPS component of the ALSM survey, operating the air and ground GPS equipment, and estimating the aircraft trajectory from the GPS observations are critical steps. We conduct ALSM surveys during periods when the Dilution of Precision (DOP) is ≤3.5 as estimated for a 15° elevation mask. We occupy ground GPS base stations that have an unobstructed sky-view down to 10°-to-15° above the horizon and are free of RF interference or significant multi-pathing. We use dual-frequency, 12-channel GPS receivers in the aircraft (Ashtech Z-12) and on the ground (Ashtech Z-12 or Trimble 4000SSi) to record data at 1Hz. The ground receivers use Dorne & Margolin chokering antennas to reduce multi-pathing and a Dorne & Margolin C146-2-1 antenna is mounted in the aircraft. All antennas have been calibrated by the National Geodetic Survey's (NGS) Geosciences Research Division. The NGS measures the antenna's L1 and L2 phase center variations as a function of GPS satellite elevation (see figure 3). Unless our GPS observations are corrected for these phase center variations, errors as large as a decimeter can be introduced into the height component of the aircraft trajectory.

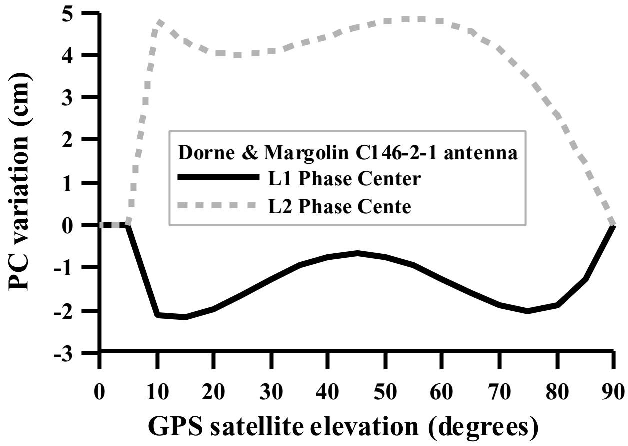

Figure 3. Phase center error as a function of satellite elevation for the C146-2-1 antenna.

We use the NGS's kinematic GPS processing software, KARS (Mader, 1992), to estimate a double-differenced, ionospherically-corrected (L3), ambiguity-fixed, phase solution for the aircraft trajectory. We use precise GPS ephemerides, computed by the International GPS Service (IGS) or the NGS, instead of the broadcast orbits in the trajectory solution.

On July 17, 2001, we mapped the Texas shoreline from Sabine Pass to Galveston Island (see figure 4). A Trimble 4000SSi receiver occupied a tide gauge benchmark at Sabine Pass and an Ashtech Z-12 occupied a tide gauge benchmark at Port Bolivar. During the almost three-hour survey, the aircraft was always within 50 km of one GPS base station, but could be as far as 150 km from the other basestation (see figure 5).

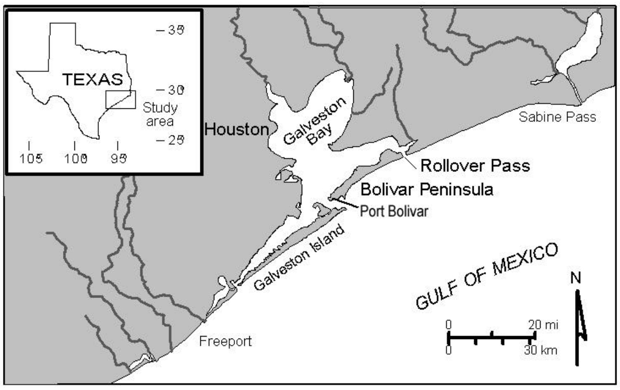

Figure 4. The Galveston Bay - Bolivar Peninsula area.

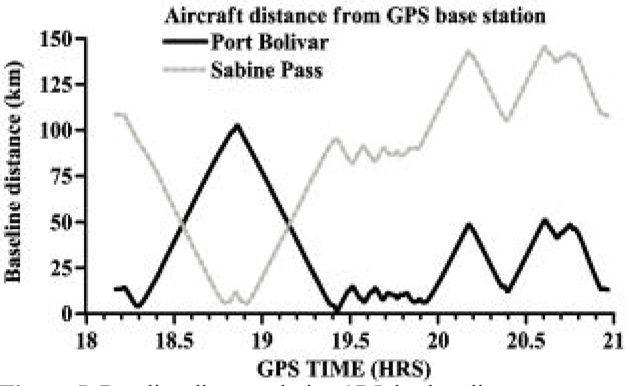

Figure 5. Baseline distance during 17 July shoreline survey.

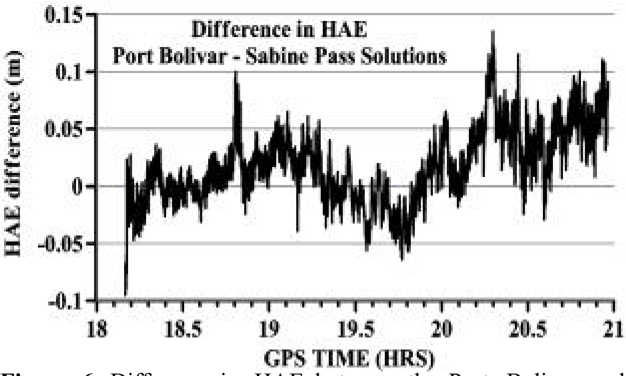

Figure 6. Difference in HAE between the Port Bolivar and Sabine Pass aircraft trajectories for July 17, 2001 shoreline survey.

We computed KARS trajectories for the aircraft using both the Port Bolivar and Sabine Pass GPS base station data. The differences between the two trajectories in the east and north, components are under 0.05m. The HAE differences between the two trajectories are under 0.05m when the aircraft is within 50km of both base stations. The HAE differences are under 0.10m even when the aircraft is more than 100 km from one of the base stations (see figure 6).

2.3 Data Coverage

Small foot-print ALSM systems operating with a 25kHz or higher laser pulse repetition rate can generate ALSM coverage with a sub-meter laser point spacing during a single pass. However, vegetation, buildings, and topography can cause shadowing that may significantly reduce the ground surface coverage. For area surveys we fly an orthogonal grid, two sets of flightlines at right angles, to minimize data gaps. Scanning from a number of different aircraft positions allows us to more accurately reconstruct the morphology of topographic or cultural features. For ALSM surveys that are route-oriented, e.g. a shoreline survey, parallel swaths can be spaced laterally so as to scan both sides of a route-parallel obstruction such as a dune line.

2.5 Ground Truth

We conduct ground GPS surveys within each ALSM survey area to acquire ground "truth" information. We re-occupy the ALSM GPS base stations and survey an open area with an unambiguous surface (road, soccer fields, large building) using kinematic GPS techniques. The ALSM data are sorted to find LIDAR points that fall within 0.5m of a ground GPS survey point. The mean elevation difference between the ALSM (last returns only) and the ground GPS are used to estimate and remove an elevation bias from the ALSM. The standard deviation of the elevation differences provide an estimate of the LIDAR precision. Selected portions from each ALSM data set (last return only) are used to generate a high-resolution (1m $\times$ 1m or 0.5m $\times$ 0.5m) digital elevation model (DEM) or laser intensity image. The kinematic GPS data are superimposed on the DEM or intensity image and examined for any horizontal mismatch.

Figure 7 is a 0.5m $\times$ 0.5m laser backscatter intensity image of the soccer field in Juticalpa, Honduras. The chalk markings on the field are discernible. On the right panel, the survey points from a GPS survey of the chalk marks and two transects across the field are superimposed on the intensity image. The GPS and ALSM match to within the resolution of the image indicating an ALSM horizontal error of <0.5m. There were 417 ALSM points that fell within 0.5m of a GPS ground survey point on the soccer field. The mean elevation difference between the GPS and ALSM was –0.169m with a RMS of 0.088m.

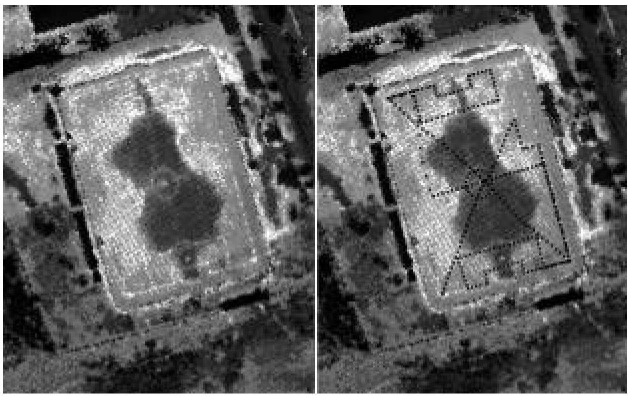

Figure 7. Intensity image of soccer field with GPS ground survey overlain.

2.4 Data classification

ALSM generates a semi-random cloud of elevation points that requires classification into reflections from ground and vegetation. As a preliminary step towards constructing digital elevation models, we have classified ALSM data using algorithms developed by TopScan GmbH (Petzold et al, 1999) and by the UT Center for Space Research (Neunschwander et al, 2000). The TopScan algorithm identifies points as either “ground” or “non-ground” by iteratively improving an initial terrain surface. The initial terrain surface is generated from the minimum value of elevation points within a large, moving window. All the elevation points that exceed a specified threshold above the terrain are classified as non-ground points and removed. Using a smaller moving window, the remaining elevation points are used to create a new terrain surface. The ALSM data are again compared to a threshold value and the non-ground points are removed. This process is repeated for a set number of iterations. The window size and threshold values are terrain-dependent and require a high level of user interaction.

The UT method classifies elevation points as ground, vegetation, or buildings using an image-based processing algorithm. The ALSM data are gridded to create a high-resolution topographic image. The average topographic surface is estimated and subtracted from the high-resolution image. The resulting residual image contains the high-frequency content of the vegetation and the building edges. The lower envelope of high-frequency residuals represents the ground surface in the signal. Using the lower envelope, an initial ground surface is estimated. A gradient-based method is used to detect and remove any large buildings remaining in the estimated ground surface. After interpolating across gaps, the final ground surface is used to classify the ALSM data. Building classification is accomplished by first detecting planar surfaces representing roofs. The building boundaries are delineated by extending the edges using a gradient-flood fill method. The building surface is then used to classify ALSM points as man-made features. A building outline can be distorted by laser multi-pathing, therefore ALSM first-returns are used for building classification.

Figure 8 is a 1m $\times$ 1m DEM constructed from first-return ALSM data of the Mayan ruins at Copan, Honduras. An aerial photograph is shown for comparison. Figure 9 is a 1m $\times$ 1m DEM of the Copan ruins constructed from last-return ALSM data filtered to remove the trees using the envelope detector and gradient based method developed at UT. The elevation points representing the Mayan archeological structures were classified and added to the ground points before the DEM was computed. For comparison is a site map constructed from a Harvard University ground survey.

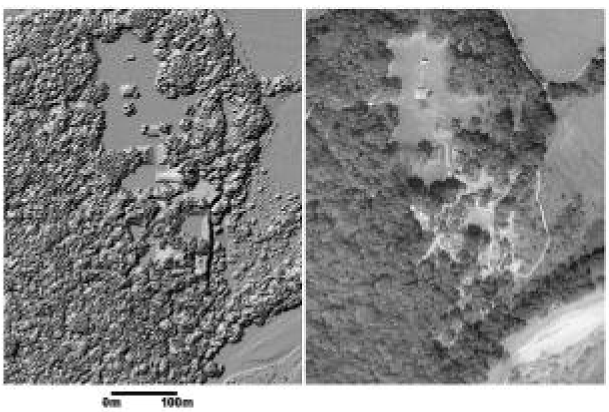

Figure 8. Left: ALSM DEM of Copan. Right: aerial photograph.

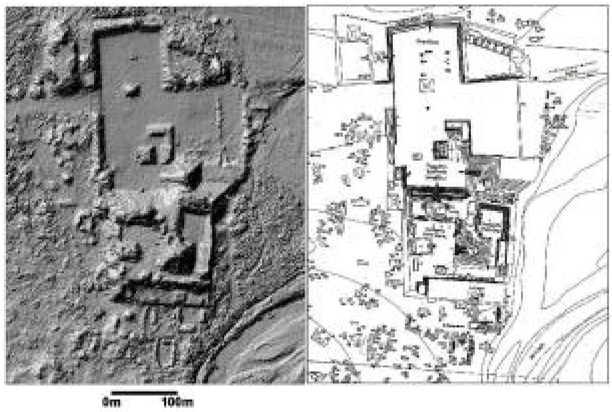

Figure 9. Left: vegetation-filtered ALSM. Right: ground survey.

3 COASTAL MAPPING

3.1 Texas Gulf Shoreline Change Project

In 1999, with the support of the Texas General Land Office, the BEG developed the Texas Shoreline Change Project. The project’s goal is to establish a state-of-the-art regional shoreline-monitoring and shoreline-change analysis program that will help solve coastal erosion and storm hazard problems along the bay and Gulf shorelines of Texas. ALSM is a key component of the Texas Shoreline Change Project; it is important in identifying "critical coastal erosion areas" and in the monitoring of historical shoreline erosion rates.

During 2000 we mapped the entire Texas Gulf shoreline using the Optech 1225 system from Sabine Pass, at the Texas-Louisiana border, to the mouth of the Rio Grande River, a distance of over 600 kilometers. We mapped the shoreline in three sections: Sabine Pass to Freeport (212km), Freeport to Corpus Christi (215km), and Corpus Christi to the Rio Grande (174km). During a typical shoreline survey, the aircraft flew two to four passes along the shoreline with parallel swaths overlapping by about 50 percent. The survey altitude varied from 450m to 760m AGL and the ground speed was usually held to 51m/sec (100 knots). The resulting ALSM coverage of the beach, dunes, and back-barrier area is 500m to 700m wide and has an average ground point spacing of <1m.

Three ground GPS receivers, Ashtech Z-12 or Trimble 4000SSi, operated during the ALSM mapping. One GPS receiver was situated at each end of the 200km section of coastline and the third was located approximately in the middle of the survey area. Six of the nine GPS base stations occupied benchmarks at NOAA or Texas Coastal Ocean Observation Network (TCOON) tide gauges. These gauges are at Sabine Pass, Port Bolivar, Port O’Connor, Port Aransas, Port Mansfield, and South Padre Island. The remaining three GPS ground stations were monuments established by either the NGS, the U.S. Army Corps of Engineers, or UT.

GPS data processing was conducted in the International Terrestrial Reference Frame 1997 (ITRF97) and the ALSM elevation points were output in Universal Transverse Mercator (UTM) coordinates and height above the GRS-80 ellipsoid (HAE). The ALSM data were compared to GPS ground surveys for the estimation of

ALSM elevation biases. Shorelines were delineated from 1m × 1m digital elevation models (DEM). Long and short ALSM ranges (e.g. clouds, birds, and multi-paths) were edited and ALSM elevation biases were removed. The edited and bias-corrected ALSM data were then imported into ARC/INFO and interpolated using the TOPOGRID module, which is based on the ANUDEM interpolation method of Hutchinson (1989). The DEM's were converted from HAE to orthometric height using the G99SSS gravimetric geoid model (Smith and Roman, 2000) and adjusted vertically so that the zero-elevation conformed to mean sea level (MSL) at the nearest tide station.

3.2 Rollover Pass

Rollover Pass is a small artificial inlet on the southeast Texas coast that connects East Bay of the Galveston Bay system with the Gulf of Mexico. The channel was dredged across a narrow portion of Bolivar Peninsula in 1954/55 and has stabilized at a width of 61m. Bolivar Peninsula is an area of naturally high erosion rates, however the shape of the shoreline shows that the artificial inlet has altered rates of shoreline movement by changing the littoral drift rate in the area.

From 1996 to 1999, Tropical Storms Josephine and Frances caused a total of 27m of scarp retreat 3.2km to the west of Rollover Pass. The process of shoreline retreat in the Rollover Pass area involves episodic and dramatic scarp retreat during storms followed by post-storm recovery and widening of the beach in front of the scarp. Eventually, the long-term erosion process resumes and the beach begins to narrow, allowing a subsequent storm to erode the scarp again.

We collected ALSM data along Bolivar Peninsula before Tropical Storm Frances on August 6, 1998, and after the storm on September 17, 1998 using an Optech 1020 ALSM system. All the HAE were transformed into orthometric heights using the National Geodetic Survey G96SSS geoid model. All the ALSM data were adjusted by –0.35m vertically so that the zero-elevation would conform to the local mean sea level as measured at the Port Bolivar tide gauge.

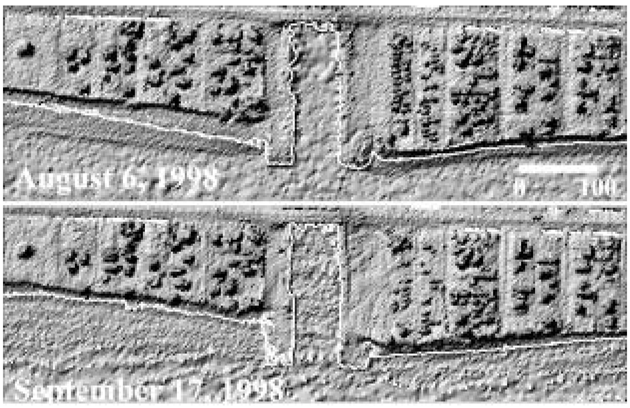

Figure 10. ALSM shaded relief images of Rollover Pass. Upper panel is the pre-Tropical Storm Frances shoreline with the 1m contour in white. The lower panel is the post-Frances shoreline.

We computed pre- and post-Frances 2m × 2m DEMs from the vertically adjusted data sets. Figure 10 shows the coastal topography at Rollover Pass before and after Frances. The 1m elevation is the white contour line on both shaded relief images. We digitized the 1m contour lines along the beach for a distance of 10km on either side of Rollover Pass. Figure 11 shows the shoreline change as represented by the movement of the 1m contour from August 6 to September 17, 1998. The shoreline data show a complex pattern of erosion. This pattern reflects the interaction of factors including offshore topography and wave refraction, piers and other man-made shoreline structures, and pre-storm beach morphology in determining the response of the beach to the storm. Except for a small area within 300m west of Rollover Pass where as much as 30m of retreat occurred, it appears that the pass had no unusual effect on beach erosion during this storm.

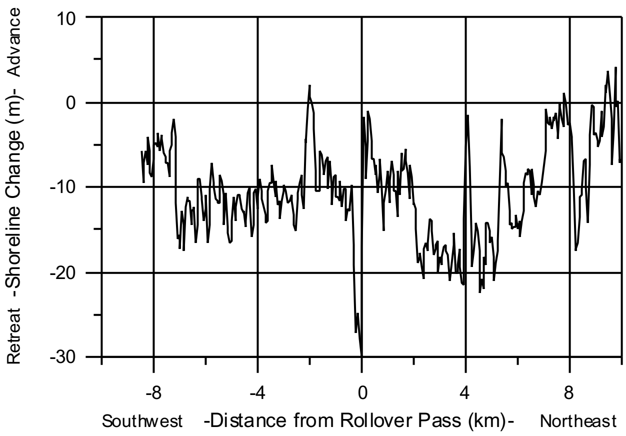

Figure 11. Change in 1m contour at Rollover Pass during due to Tropical storm Frances.

Figure 12. Geotube installed in front of the beach scarp at Bolivar Peninsula during July 2001

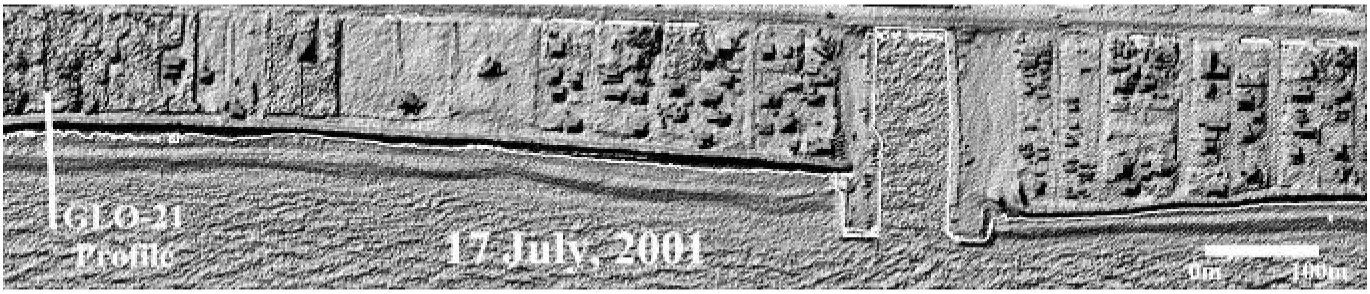

Figure 13. ALSM shaded relief image of Rollover Pass on 17 July 20001 showing geotubes installed behind the beach and in front of the eroding beach scarp. The 1m elevation contour is shown in white. A shore-normal beach profile (GLO-21) is to the left of Rollover Pass.

In 1999, communities on Galveston Island and Bolivar Peninsula began installing geotextile tubes (geotubes) along the most erosion-prone stretches of shoreline. The geotubes are sand-filled sleeves of geotextile fabric with an approximately 4m oval cross section (see figure 12). The ALTM 1225 system was used to map the Galveston and Bolivar shorelines, including the geotubes, on 17 and 18 July, 2001 (see figure 13).

Kinematic GPS and a total station were used to measure a set of shore-normal profiles after the ALSM surveys were flown. The profiles extended across the geotubes, the beach, and for 100-200m offshore. Figure 14 compares the topography measured by ALSM with the total station profile at location GLO-21 (see figure 13). The ALSM elevations agree well with the ground control except were dense vegetation behind the geotubes masks the true ground surface. Thick deposits of sargassum on the back-beach also cause the ALSM elevations to be slightly higher than the true ground surface. These new data will be used to study the response of the beach and geotubes to coastal processes.

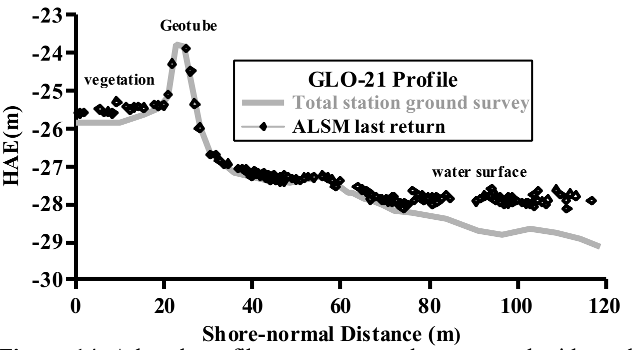

Figure 14. A beach profile across a geotube measured with total station on 19 July, 2001 is compared to ALSM data collected on 17 July, 2001.

4 FLOOD HAZARD MAPPING

4.1 Hurricane Mitch

From October 27 to November 1, 1998, Central America was devastated by Mitch, a category 5 hurricane on the Saffir-Simpson scale with winds up to 155 mph. Mitch is responsible for over nine thousand deaths, making it one of the deadliest Atlantic tropical cyclones in history and comparable to the great Galveston storm of 1900. In Honduras, the human toll is an estimated 5,000 deaths. Whole villages were washed away and an estimated 70-to-80 percent of the transportation infrastructure was destroyed. At least 70 percent of the crops were destroyed; an estimated $900 million loss. Honduras is still rebuilding the housing and infrastructure destroyed by Hurricane Mitch. To minimize future flood disasters, the Honduran government needs maps that accurately delineate probable areas of inundation by flooding.

From February to March 2000, the BEG, the U.S. Geological Survey (USGS) and Optech collaborated to map the channel geometry of the floodplains within 15 Honduran municipalities using ALSM. Between January 7-21, 2001, the USGS and BEG collaborated again to measure the geometry and location of 21 bridges in these 15 municipalities using a total station and GPS equipment. The USGS will use the bridge geometry and ALSM data to generate new, accurate 50-year flood inundation maps for each Honduran municipality.

The construction of the Honduran inundation maps involved three general steps. We estimated the 50-year stream discharges for the rivers in each municipality using a statistical analysis of precipitation and a rainfall-runoff model. We then computed water-surface elevations using channel geometry information from ALSM-derived DEM's and the HEC-RAS hydraulic simulation model (U.S. Corps of Engineers, 1998). HEC-GeoRAS, an ArcView extension, was used to define the stream thalweg, banks, overbank centerlines, and extract channel cross-sections from the DEM's (U.S. Corps of Engineers, 2000). Often a shaded relief image of the DEM was used as background to help locate these various lines. Manning roughness coefficients, ***n***, were estimated by the hydrologists from field observations or by reviewing a shaded relief image of the DEM. The shaded relief image gave a good view of the density of vegetation in the stream channel – the higher densities were given higher ***n*** values. Finally, the simulated water levels from the hydraulic mode were plotted as depth and area of inundation over the DEM.

4.2 Tegucigalpa

We installed the ALTM 1225 system in a Beech King Air A-90 aircraft in the U.S. and ferried the aircraft to Toncontin Airport in Tegucigalpa, Honduras. Tegucigalpa was mapped during 1-2 March, 2000. We operated the instrument at a laser repetition rate of 25kHz, a laser scanning rate of 28Hz, and a laser scan angle of ±20° off nadir. We flew the aircraft at an average airspeed of 140 knots (72 m/s). This resulted in a spacing of about 2.6m between laser scan lines. The aircraft altitude varied between 800m to 1200m above ground level (AGL). To generate an approximately 1m × 1m ground point spacing, we mapped the city with a grid of orthogonal flight lines with approximately 30 percent side-lap between adjacent swaths (see figure 15).

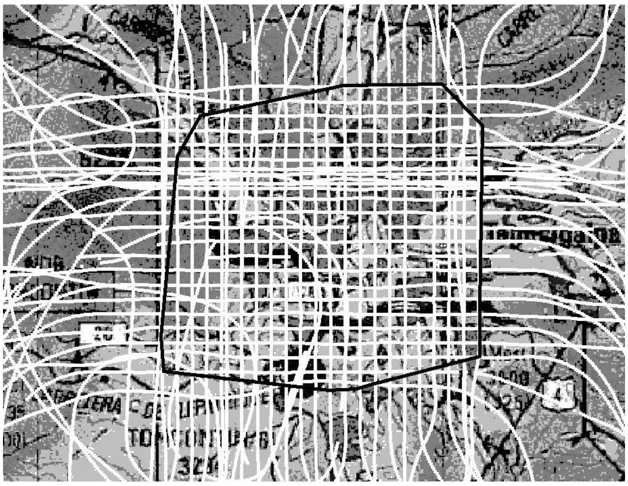

Figure 15. Flightlines over the 10 km x 10 km survey area for Tegucigalpa, Honduras.

These flights produced a uniform and dense ALSM data point coverage over an approximately 10km × 10km area of Tegucigalpa. Figure 16 shows the point "cloud" distribution over the city center at the confluence of the Rio Grande O Choluteca and the Rio Guacerique. The only data gaps are on the rivers where the water surface was often too specular to provide good laser returns.

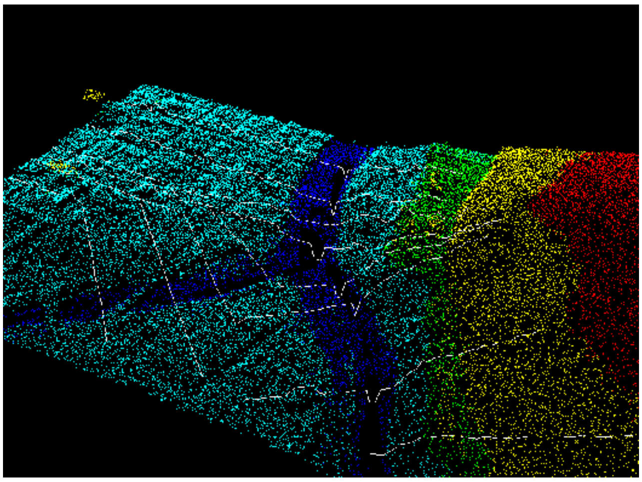

Figure 16. ALSM point cloud for central Tegucigalpa. The individual laser returns are colored to represent elevation. Channel cross-sections are shown in white.

We edited the ALSM data, compared them to ground surveys, and corrected for elevation biases. We generated a 1.5m × 1.5m "all points" DEM using all the ALSM last-return data. We then applied the TopScan vegetation-filtering algorithm to the last-return ALSM data. The filter parameters were chosen so that reflections from trees were removed, but most reflections from the ground surface and buildings were retained. We constructed a second, 1.5m × 1.5m "vegetation-removed" DEM from the filtered ALSM data. We then used HEC-GeoRAS to define the river channels and extract cross-sections from the "vegetation-removed" DEM' (see figure 16).

Heavy rains associated with Hurricane Mitch caused three major landslides in Tegucigalpa. The most devastating slide occurred on the Cerro Berrinche in northwest Tegucigalpa. The El Berrinche landslide destroyed an entire hillside community and dammed the Rio Grande O Choluteca causing significant flooding in the city center. Figure 17 shows the topography of the El Berrinche landslide after mitigation. The toe of the landslide has been cut into a series of steps and stabilized with gabions.

Figure 17. Shaded relief image of the El Berrinche landslide in Tegucigalpa.

5 DISCUSSION

Erosion along the Texas coast caused by the recent tropical storms in the Gulf of Mexico has intensified efforts to save property and houses. ALSM can provide the topographic models needed for geomorphic analysis and the delineation of areas particularly susceptible to storm damage. Post-storm ALSM surveys allow rapid and quantitative assessment of the amount of erosion and vulnerability of the coast to subsequent storms. In the past, coastal geologists and engineers have either conducted regional studies with sparse data or local studies with detailed data. With ALSM, however, it is possible to acquire detailed and accurate topographic data over a broad coastal region allowing geomorphic analysis across the continuum of spatial scales.

Landslide and flooding risks are strongly dependent on topography. With ALSM it is possible to characterize topography over large areas with sufficient resolution and accuracy to model hydrologic and geomorphic processes with unprecedented detail. New, quantitative models for hydrologic and surficial processes can be developed and tested using high-resolution topographic data.

6 REFERENCES

Blair, J.B., D. L. Rabine, and M. A. Hofton, 1999, The Laser Vegetation Imaging Sensor: a medium-altitude, digitization-only, airborne laser altimeter for mapping vegetation and topography, ISPRS Journal of Photogrammetry and Remote Sensing, vol. 54, no.2-3, pp.115-122.

Burman, H., 2000, Adjustment of laser scanner data for correction of orientation errors, International Archives of

Photogrammetry and Remote Sensing, Vol. 23, Part B3, pp.125-132.

Gutiérrez, R., J. C. Gibeaut, M. M. Crawford, M. Mahoney, S. Smith, W. Gutelius, D. Carswell, and E. MacPherson, 1998, Airborne laser swath mapping of Galveston Island and Bolivar Peninsula, Texas, in Proceedings of the Fifth International Conference for Remote Sensing for Marine and Coastal Environments, San Diego, CA., vol. I, pp. 236-243.

Harding, D.J., J.B. Blair, D.L. Rabine, and K.L. Still, 2000, SLICER airborne laser altimeter characterization of canopy structure and sub-canopy topography for the BOREAS Northern and Southern Study Regions: Instrument and Data Product Description, Volume 93 in Technical Report Series on the Boreal Ecosystem-Atmosphere Study (BOREAS), F.G. Hall and J. Nickeson, Eds., NASA/TM-2000-209891, Vol. 93, 45 pp.

Hutchinson M.F., 1989, A new procedure for gridding elevation and stream line data with automatic removal of spurious pits, Journal of Hydrology, vol.106, pp211-232.

Krabill, W.B., R.H. Thomas, C.F. Martin, R.N. Swift, and E.B. Frederick, 1995; Accuracy of Airborne Laser Altimetry Over the Greenland Ice Sheet, International Journal Remote Sensing, Vol. 16, No. 7, pp. 1211-1222.

Krabill, W., W. Abdalati, E. Fredrick, S. Manizade, C. Martin, J. Sonntag, R. Swift, R. Thomas, W. Wright, J. Yungel, 2000, Greenland Ice sheet: high–elevation balance and peripheral thinning, Science, pp.428-430.

Mader, G. L., 1992, Rapid static and kinematic Global Positioning System solutions using the ambiguity function techniqu*e*, Journal of Geophysical Research, vol. 97(B3): pp.3271-3283.

Neunschwander, A., M. Crawford, C. Weed, and R. Gutierrez, 2000, Extraction of digital elevation models for airborne laser terrain mapping data, Geosciences and Remote Sensing Symposium, 2000, Proceedings, IGARSS 2000, IEEE 2000 International, vol.5, pp.2305-2307.

Petzold, B., P. Reiss, and W. Stössel, 1999, Laser scanning – surveying and mapping agencies are using a new techniques for the derivation of digital terrain models, ISPRS Journal of Photogrammetry and Remote Sensing, vol. 54, no.2-3, pp.95-104.

Rabine, D. L., J. L. Bufton, and C. R. Vaughn, 1996, Development and test of a raster scanning laser altimeter for high-resolution airborne measurements of topography, IGARSS96.

Smith, D.A., and D.R. Roman, 2001, GEOID99 and G99SSS: One arc-minute models for the United States, Journal of Geodesy, in press.

Wehr, A. and U. Lohr, 1999, Airborne laser scanning - an introduction and overview, ISPRS Journal of Photogrammetry and Remote Sensing, vol. 54, no.2-3, pp.68-82.

U.S. Corps of Engineers, 1998, HEC-RAS River Analysis System, Hydraulic Reference Manual version 2.2, Hydraulic Engineering Center, Davis, California, 237p.

U.S. Corps of Engineers, 2000, HEC-GeoRAS, An extension for support of HEC-RAS using ArcView, User’s Manual version 2.2, Hydraulic Engineering Center, Davis, California, 96p.